HOW DO APERTURE SIZES IN LIMESTONE VARY FOR THE ONSETS OF TURBULENT FLOW AND FIRST-ORDER DISSOLUTION KINETICS?

Trevor Faulkner
Limestone Research Group, Geography, Earth and Environmental Sciences, University of Birmingham, Edgbaston, Birmingham, B15 2TT, UK, trevor@marblecaves.org.uk

It is commonly stated in the literature that the "breakthrough" point at the transition from slow high-order to fast first-order dissolution kinetics in limestone occurs at an exit aperture of about one centimetre, and that this coincides with the transition from a wholly laminar flow to a turbulent flow. These relationships are approximately true for a range of conduit geometries in sub-horizontally bedded strata. However, the exit aperture for the onset of turbulence varies with the hydraulic gradient whereas the exit aperture for the onset of first-order kinetics varies with the hydraulic ratio, which is the hydraulic gradient divided by the path length. These transitions only occur at the same exit aperture for planar fissures and cylindrical tubes of lengths 290 m and 452 m. Breakthrough can occur before or after the onset of turbulence. Aperture sizes for breakthrough and turbulence can be over a metre for long and shallow conduits but sub millimetre for short and steep conduits. This paper analyses these relationships for many conduits in natural and artificial conditions and discusses their relevance to the multitude of possible karst situations, where hydraulic ratios can be considered over 17 orders of magnitude.

1. Introduction

The physics and chemistry of limestone dissolution along planar fissures and cylindrical conduits were derived in two key papers over twenty years ago by Dreybrodt (1990) and Palmer (1991). These built on important earlier works, including those by Weyl (1958), Bögli (1964), White (1977) and Palmer (1981). A later treatise to present detailed (and animated) models of speleogenesis based on the principles of the Palmer / Dreybrodt model is that by Dreybrodt et al. (2005). Palmer (1991: Eq. 6) showed that when water flows past any point in a conduit in natural limestone, the rate of solutional wall retreat (S) is:

$$S = 31.56k_n(1/\rho)(1 - C/C_s)^n \text{ cm per year,}$$

where k_n mg-cm L^{-1} s^{-1} is the appropriate reaction coefficient, ρ gm cm^{-3} is the density of the limestone, C gm cm^{-3} is the point concentration of calcite in solution, C_s gm cm^{-3} is the appropriate saturation concentration of calcite and n is the reaction order. k_n, C and C_s vary with temperature and P_{CO2} levels. $k_{n>1}$ also varies with C/C_s, and C also varies with the geometrical and hydrological parameters of the conduit. Dissolution when the solution is well below saturation occurs at a fast "first-order kinetics" rate, where n = 1. At the beginning of the conduit, C is at a minimum, and may be close to zero for an allogenic stream running from non-carbonate rocks. In this case, dissolution at the entrance is at the appropriate maximum rate of $S_{max} = 31.56k_1/\rho$ cm a^{-1}. The calcite concentration increases downstream from the entry point. If C approaches C_s, the dissolution rate becomes small and the reaction proceeds with "higher-order kinetics" as the flow continues. The change occurs near a point along the conduit that Weyl (1958) called the "penetration length", where $0.6 < C/C_S < 0.9$, dependent on temperature and P_{CO2}. Beyond here, $n \geq 4$, governed by non-calcitic impurities, and "mixing corrosion" (Bögli 1964) can be important if sustained over long geological timescales. The Palmer/Dreybrodt model quantifies the gradual conduit enlargement under slow high-order kinetics as the penetration length slowly increases. When it reaches to the exit of the aperture, there is a "kinetic trigger" (White 1977) and dissolution then occurs at the applicable maximum first-order rate over the whole length of the flow path, to create a conduit with a near-uniform cross-section. This important event in karst evolution is called the "breakthrough point" (Dreybrodt 1990). If limestone comprised pure calcite, the penetration length might not increase and caves would then only form if initial fracture geometries allowed immediate first-order dissolution kinetics, i.e. "tectonic inception" (Faulkner 2006a; 2006b). When C/C_s becomes < c. 60 %, "breakthrough behaviour" dominates and mixing corrosion is unimportant (Romanov et al. 2003). At 10 °C and with the inflowing water containing 1 % CO_2, $S_{max} \approx 1$ mm per year (Palmer 1991), although even faster dissolution rates seem possible in water that is extremely unsaturated (e.g., Palmer 1991: Fig. 8). Wall retreat rates may also be increased by mechanical erosion, which is lithology dependent and amplified in turbulent flow. White (1977) pointed out that the kinetic trigger can occur at an exit aperture of 1–10 mm, a range that has been widely quoted. He also stated that this coincides approximately with the size at which wholly laminar flow starts to become turbulent (without there being a causal relationship), and this "coincidence" has also been widely assumed. This paper analyses these relationships and discusses their relevance to the multitude of possible karst situations.

Flow rates, water velocities and the transition to turbulent flow in conduits are controlled by the hydraulic gradient (HG; Head / path length = H/L), among other variables. The main parameters at the chemical breakthrough point are controlled by a geometrical variable called the "hydraulic ratio", which equals the hydraulic gradient divided by the path length (HR; H/L^2; Dreybrodt 1990). The necessity for the extra divisor can be understood, because dissolution always proceeds along the whole path length. Based on the work of Palmer (1991), which itself was based on the Hagen-Poiseuille Equations for laminar flow, these relationships were plotted graphically by Faulkner (2006a: Fig. 3). Those curves illustrated the linear relationships among the logarithms of hydraulic conductivity, water

velocity, flow rate, hydraulic ratio and the exit apertures at the breakthrough point for both wide planar fissures and circular tubes of lengths 1–1,000 m. Also shown were the applicable Reynolds numbers (see below) for each flow regime. Some of these relationships are presented in Table 1 and illustrated in a modified format in Figure 1. This plots the minimum fissure exit aperture or tube radius in centimetres for the establishment of first-order kinetics, plus the minimum conduit size for the onset of turbulent flow, against the hydraulic gradient of the conduit. Logarithmic scales are used in Figure 1, with the axes values chosen to exceed the extreme ranges likely to apply in natural and artificial karst systems. The minimum conduit sizes for the onset of turbulent flow vary with cross-section shape, but are independent of conduit length for uniform conduits. Those for the chemical breakthrough point vary with conduit shape as well, but also vary with length; they are shown for five set lengths from 1–10,000 m.

Table 1. Fissure and tube sizes for the onsets of turbulence and first-order kinetics for various lengths and hydraulic gradients.

Length L	Hydraulic gradient H/L	Aperture $w_t = 0.1663 * HG^{-½}$	Radius $r_t = 0.1153 * HG^{-½}$	Hydraulic Ratio (HR) H/L^2	$\log w_{fo} = -(4.80 + \log HR)/3$	Aperture w_{fo}	$\log r_{fo} = -(5.47 + \log HR)/3$	Radius r_{fo}
m	HG	cm	cm	m^{-1}		cm		cm
10,000	1.00E-09	166.1907	115.2344	1.00E-13	2.7333	541.1695	2.5100	323.5937
1,000	1.00E-08	77.1448	53.4912	1.00E-11	2.0667	116.5914	1.8433	69.7161
100	1.00E-07	35.8102	24.8303	1.00E-09	1.4000	25.1189	1.1767	15.0199
10	1.00E-06	16.6229	11.5261	1.00E-07	0.7333	5.4117	0.5100	3.2359
1	1.00E-05	7.7163	5.3503	1.00E-05	0.0667	1.1659	-0.1567	0.6972
10,000	1.00E-08	77.1448	53.4912	1.00E-12	2.4000	251.1886	2.1767	150.1989
1,000	1.00E-07	35.8102	24.8303	1.00E-10	1.7333	54.1170	1.5100	32.3594
100	1.00E-06	16.6229	11.5261	1.00E-08	1.0667	11.6591	0.8433	6.9716
10	1.00E-05	7.7163	5.3503	1.00E-06	0.4000	2.5119	0.1767	1.5020
1	1.00E-04	3.5818	2.4836	1.00E-04	-0.2667	0.5412	-0.4900	0.3236
10,000	1.00E-07	35.8102	24.8303	1.00E-11	2.0667	116.5914	1.8433	69.7161
1,000	1.00E-06	16.6229	11.5261	1.00E-09	1.4000	25.1189	1.1767	15.0199
100	1.00E-05	7.7163	5.3503	1.00E-07	0.7333	5.4117	0.5100	3.2359
10	1.00E-04	3.5818	2.4836	1.00E-05	0.0667	1.1659	-0.1567	0.6972
1	1.00E-03	1.6627	1.1529	1.00E-03	-0.6000	0.2512	-0.8233	0.1502
10,000	1.00E-06	16.6229	11.5261	1.00E-10	1.7333	54.1170	1.5100	32.3594
1,000	1.00E-05	7.7163	5.3503	1.00E-08	1.0667	11.6591	0.8433	6.9716
100	1.00E-04	3.5818	2.4836	1.00E-06	0.4000	2.5119	0.1767	1.5020
10	1.00E-03	1.6627	1.1529	1.00E-04	-0.2667	0.5412	-0.4900	0.3236
1	1.00E-02	0.7718	0.5352	1.00E-02	-0.9333	0.1166	-1.1567	0.0697
10,000	1.00E-05	7.7163	5.3503	1.00E-09	1.4000	25.1189	1.1767	15.0199
1,000	1.00E-04	3.5818	2.4836	1.00E-07	0.7333	5.4117	0.5100	3.2359
100	1.00E-03	1.6627	1.1529	1.00E-05	0.0667	1.1659	-0.1567	0.6972
10	1.00E-02	0.7718	0.5352	1.00E-03	-0.6000	0.2512	-0.8233	0.1502
1	1.00E-01	0.3583	0.2484	1.00E-01	-1.2667	0.0541	-1.4900	0.0324
10,000	1.00E-04	3.5818	2.4836	1.00E-08	1.0667	11.6591	0.8433	6.9716
1,000	1.00E-03	1.6627	1.1529	1.00E-06	0.4000	2.5119	0.1767	1.5020
100	1.00E-02	0.7718	0.5352	1.00E-04	-0.2667	0.5412	-0.4900	0.3236
10	1.00E-01	0.3583	0.2484	1.00E-02	-0.9333	0.1166	-1.1567	0.0697
1	1.00E+00	0.1663	0.1153	1.00E+00	-1.6000	0.0251	-1.8233	0.0150
10,000	1.00E-03	1.6627	1.1529	1.00E-07	0.7333	5.4117	0.5100	3.2359
1,000	1.00E-02	0.7718	0.5352	1.00E-05	0.0667	1.1659	-0.1567	0.6972
100	1.00E-01	0.3583	0.2484	1.00E-03	-0.6000	0.2512	-0.8233	0.1502
10	1.00E+00	0.1663	0.1153	1.00E-01	-1.2667	0.0541	-1.4900	0.0324
1	1.00E+01	0.0772	0.0535	1.00E+01	-1.9333	0.0117	-2.1567	0.0070
10,000	1.00E-02	0.7718	0.5352	1.00E-06	0.4000	2.5119	0.1767	1.5020
1,000	1.00E-01	0.3583	0.2484	1.00E-04	-0.2667	0.5412	-0.4900	0.3236
100	1.00E+00	0.1663	0.1153	1.00E-02	-0.9333	0.1166	-1.1567	0.0697
10	1.00E+01	0.0772	0.0535	1.00E+00	-1.6000	0.0251	-1.8233	0.0150
1	1.00E+02	0.0358	0.0248	1.00E+02	-2.2667	0.0054	-2.4900	0.0032
10,000	1.00E-01	0.3583	0.2484	1.00E-05	0.0667	1.1659	-0.1567	0.6972
1,000	1.00E+00	0.1663	0.1153	1.00E-03	-0.6000	0.2512	-0.8233	0.1502
100	1.00E+01	0.0772	0.0535	1.00E-01	-1.2667	0.0541	-1.4900	0.0324
10	1.00E+02	0.0358	0.0248	1.00E+01	-1.9333	0.0117	-2.1567	0.0070
1	1.00E+03	0.0166	0.0115	1.00E+03	-2.6000	0.0025	-2.8233	0.0015
10,000	1.00E+00	0.1663	0.1153	1.00E-04	-0.2667	0.5412	-0.4900	0.3236
1,000	1.00E+01	0.0772	0.0535	1.00E-02	-0.9333	0.1166	-1.1567	0.0697
100	1.00E+02	0.0358	0.0248	1.00E+00	-1.6000	0.0251	-1.8233	0.0150
10	1.00E+03	0.0166	0.0115	1.00E+02	-2.2667	0.0054	-2.4900	0.0032
1	1.00E+04	0.0077	0.0054	1.00E+04	-2.9333	0.0012	-3.1567	0.0007

2. Onset of turbulent flow

By convention, dimensionless Reynolds Numbers (R_e) are used to characterise flow regimes in fissures and pipes. These are commonly defined as: $R_e = w\rho V/\mu$ (fissure) and $R_e = 2r\rho V/\mu$ (tube), where w cm = aperture width of a fissure, r cm = radius of a cylindrical tube, ρ = the density of the water = 1gm cm^{-3}, V cm sec^{-1} = its mean velocity and μ = its dynamic viscosity = 0.01307 gm cm^{-1} sec^{-1} at 10 °C (Ford and Williams 2007: p112).

Laminar flows in fissures and tubes obey the Hagen-Poiseuille Equations: $V = w^2\rho g^*HG/12\mu$ (fissure) and $V = r^2\rho g^*HG/8\mu$ (tube), by re-arrangement of Palmer (1991: Eq. 3), where g = 981 cm sec^{-2} is the gravitational acceleration, HG = Hydraulic Gradient. Normally, $0 \leq HG \leq 1$, which is the normal maximum for vertical flow paths under subaerial conditions. $HG > 1$ is possible for inlets submerged beneath a reservoir or lake.

The above equations can be re-arranged to state the applicable aperture and radius in terms of the Reynolds Number:

$w = [12\mu^2 R_e/(\rho^2 g^*HG)]^{⅓}$ cm (fissure) and

$r = [4\mu^2 R_e/(\rho^2 g^*HG)]^{⅓}$ cm (tube).

The value of R_e at which flows in karst conduits start to become turbulent is assumed to be 2,200 (Kaufmann and Braun 1999). Substituting this value and the other given constants into these equations gives: $w_t = 0.1663(HG)^{-⅓}$ cm (fissure) and $r_t = 0.1153(HG)^{-⅓}$ cm (tube), where w_t and r_t are the minimum aperture or radius for the onset of turbulent flow in fissures or tubes in limestone. Two plots in Figure 1 show how these vary from 166 cm or 115 cm at $HG = 10^{-9}$ via 0.018 cm or 0.012 cm at $HG = 10^0$ to 0.008 cm or 0.005 cm at $HG = 10^4$.

3. Onset of first-order kinetics

The approximate fissure aperture (w_{fo}) and tube radius (r_{fo}) at the breakthrough point at 10 °C with 1% P_{CO2} for an unsaturated input stream (i.e. C_0 = 0 gm $CaCO_3$ cm^{-3}) were derived by Faulkner (2006a) from the discussion by Palmer (1991: p8 and Figs. 12a and 12b). These gave: $\log w_{fo} = \log r_{fo} = -(5 + \log HR)/3$, where HR m^{-1} = the hydraulic ratio and the path length L is measured in metres. However, more accurate derivations are: $\log w_{fo} = -(4.80 + \log HR)/3$ and $\log r_{fo} = -(5.47 + \log HR)/3$, which are used to generate five length plots in Figure 1 for both fissures and tubes. These show how the aperture or radius required vary from 541 cm or 324 cm for a 10 km flow route with $HG = 10^{-9}$ and $HR = 10^{-13}$ m^{-1} via 0.12 cm or 0.08 cm for a 100 m length with $HG = 10^0$ and $HR = 10^{-2}$ m^{-1} to 0.0012 cm or 0.0007 cm for a 1 m length with $HG = 10^4$ and $HR = 10^4$ m^{-1}.

4. Coincidence of turbulence and breakthrough

The onsets of turbulent flow and first-order kinetics coincide at the same conduit sizes if: $w_t = w_{fo}$ (fissures) or $r_t = r_{fo}$ (tubes), i.e. if: $\log w_t = \log[0.1663(HG)^{-⅓}] = -(4.80 + \log HR)/3$ or if: $\log r_t = \log[0.1153(HG)^{-⅓}] = -(5.47 + \log HR)/3$.

Noting that HR = HG/L, these relationships simplify at coincidence to L = 290 m (fissures) and L = 452 m (tubes), for any hydraulic gradient and its related conduit size. Because 100 m-long fissures have a similar aperture at breakthrough as the radius of a 100 m-long tube at the onset of turbulence for each HG, and 1,000 m-long fissures have a similar aperture at the onset of turbulence as the radius of a 1,000 m-long tube at breakthrough, these two pairs of curves almost coincide on Figure 1.

5. Discussion

Karst hydrologists state that hydraulic gradients commonly occur in the range 10^{-2} to 10^{-4} for karst aquifers in sub-horizontal sedimentary limestones (e.g., White 1988: p165). From Figure 1, the breakthrough point in a 100 m-long fissure or tube occurs when the aperture or radius reaches 0.54–2.51 cm or 0.32–1.50 cm over this HG range. For 1,000 m- and 10,000 m-long flow routes, the required sizes increase to 1.17–5.41 cm or 0.70–3.24 cm and 2.51–11.66 cm or 1.50–6.97 cm. However, for long flow paths with $HG \leq 10^{-4}$, they can increase up to several metres. For steep flows with $10^{-2} \leq HG \leq 10^0$, they can reduce to < 1 mm. For fissures or tubes that are < 290 m or < 452 m long at any HG, the onset of turbulent flow occurs after their exit widths or radii reach their breakthrough sizes, but will be gained under fast first-order kinetics. For conduits longer than those lengths, turbulence starts before breakthrough is achieved. The Palmer/Dreybrodt analysis applies only for laminar flow. For each conduit size, turbulence reduces the mean velocity and discharge rate. Hence, for these longer conduits, the onset of first-order dissolution is delayed and might only be achieved at larger aperture sizes than shown. Beyond the "central" ranges of HG from 10^{-2} to 10^{-4} and L from 100–1,000 m, Figure 1 illustrates the applicable breakthrough points and onsets of turbulence at the extreme limits of both natural and artificial practical situations, as discussed below.

6. Breakthrough time

Dreybrodt (1990) and Palmer (1991) presented similar equations to represent T_B, the time taken for a planar fissure with an initial aperture of w_0 to achieve breakthrough. A simplified form of Palmer (1991: Eq. 8) is: $T_B = \text{constant}^* w_0^{-3.12} * (HR)^{-1.37}$ years, where the constant varies with temperature and the P_{CO2} of the input stream. Palmer (1991: Fig. 13) plotted T_B against HR for various w_0 from 0.001–0.1 cm for $1{,}000{,}000 \geq T_B \geq 100$ years. For $T_B < 100$ years, the linear relationships on log-log scales breakdown, reaching $T_B = 0$ for conditions at tectonic inception (Faulkner 2006a: Fig. 5). Hence, there is a wide range of breakthrough times in natural karst systems that vary with hydraulic gradient, conduit length and initial aperture.

7. Diagenesis

Limestone is commonly formed by carbonate deposition in shallow tropical or deep marine environments, followed by

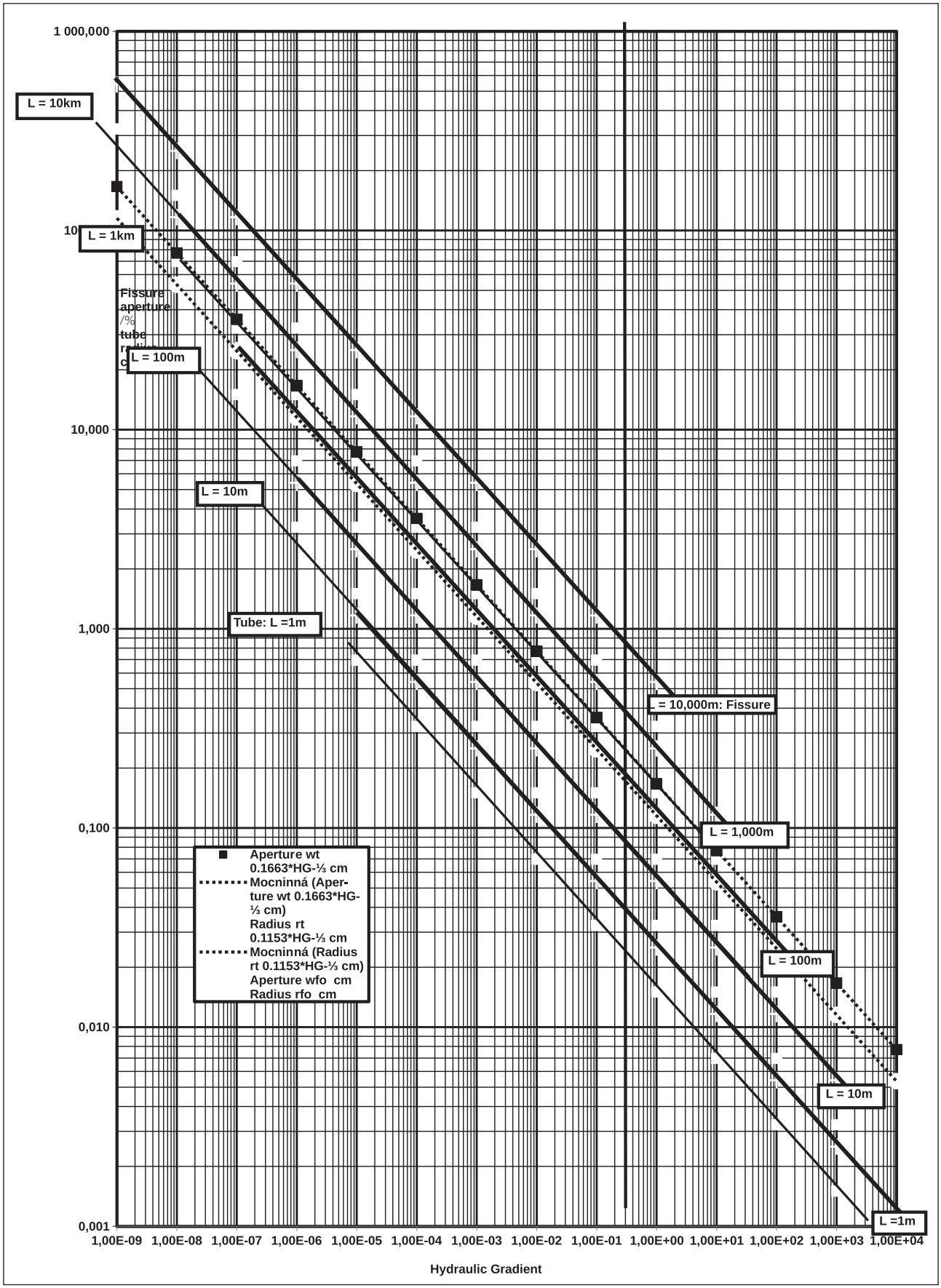

Figure 1. Minimum fissure aperture (wt or wfo) and tube radius (rt or rfo) in cm for the onset of turbulent flow or first order dissolution kinetics at 10 °C and 1% PCO2, plotted against hydraulic gradient (HG). wt (dashed lines) and rt (dotted lines) are independent of path length. wfo and rfo (solid lines) are shown for path lengths of 1 m, 10 m, 100 m, 1,000 m and 10,000 m. The vertical line indicates the maximum HG of 1, for vertical flow paths under normal subaerial conditions. For karst submerged by a reservoir or lake, HG can be >1.

compaction, lithification, and diagenesis in partly meteoric waters. During diagenesis, apertures are at the scale of the pores between crystals, orders of magnitude below values in Figure 1, so that chemical breakthrough does not apply.

8. Long drainage basins

Following exhumation and uplift, initial flows in homogeneous non-fractured limestone would be along inception horizons, perhaps in an adjacent more permeable lithology (Lowe and Gunn 1997). Apertures commonly remain at the pore scale, so that breakthrough is still not possible, even with short vertical flow paths, until high-order dissolution eventually creates conduits with w > 0.001 cm. For example, for long "shallow" karst aquifers, i.e. those ≥ 1 km in length with HG ≤ 10^{-2}, chemical breakthrough does not occur until the conduit reaches over 1 cm in size. From Palmer (1991: Fig. 13), this would take over one million years, if the initial aperture was 0.01 cm.

For long fractured limestone aquifers, the flow route might reach deep below the surface and even pass through non-calcitic lithologies before rising to the resurgence. Because natural fractures tend to reduce in size with depth and the rock temperature increases, the flow would follow a path through apertures of varying initial size at varying temperatures, with the possible addition of strong acid dissolution. The effect on breakthrough times is much more complex. This is the realm of hypogene speleogenesis (Klimchouk 2007), where this new science still requires considerable analysis and quantification (Faulkner 2007a).

9. Shorter drainage routes

The initial apertures of shorter fracture networks probably lie in the range 0.001–0.1 cm. From Figure 1, only those short flow paths with L < 10 m, w > 0.01 cm and HG > 10^{-2} could exhibit breakthrough behaviour. However, fractures in the "common" HG range $10^{-2} – 10^{-4}$ with 1.0 cm > w > 0.1 cm (which may apply close to the surface) could be at breakthrough for L < 1,000 m.

10. Tall vertical fractures

It is conceivable that limestone cliffs, including any ≥ 1 km high, could have vertical fracture systems that reach from the cliff top to the cliff base. Water percolating down such fractures at HG = 1 would reach the breakthrough point at an aperture of 0.25 cm, if there is enough recharge to keep the fissure filled with water. For shorter cliffs, the required apertures are smaller. This explains the numerous marble cave entrances located near valley shoulders in Central Scandinavia (Faulkner 2005).

11. Epikarst joints and limestone pavements

In the epikarst, water-filled vertical joints ≤ 10 m high that transmit water into a lower vadose zone would need apertures of only 0.05 cm to achieve first-order kinetic dissolution. This is the place where joint openings are naturally the largest, from surface stress relief and other processes. Hence, breakthrough is reached quickly here, or even immediately on the opening of a joint, if it is large enough for tectonic inception. This explains the epikarst phenomenon, where cave entrance passages can be showered with water during heavy rain. Similarly, new dolines can form rapidly in abandoned limestone quarries (Gunn and Gagen 1987). Vertical grikes ≤ 1 m deep are common in limestone pavements. They achieve fast dissolution with apertures of 0.025 cm, making tectonic inception even more likely here. Smooth pavements under continuous rainfall would lower up to 0.5 mm per year by dissolution, best exemplified by 1.5 m of marble erosion in the Holocene at Madre de Dios, Chile (Faulkner 2009).

12. Speleothem dripwaters

Speleothem deposition occurs when dissolved calcite precipitates by CO_2 vigorously degassing in cave air, where the dripwater flow reaches an open passage roof or wall. If autogenic water at 10 °C seeps through a non-carbonate rock with P_{CO2} of 1 % derived from overlying soils, it will contain little dissolved calcite before entering the limestone, but will then reach calcite saturation in closed conditions at 50 mg L^{-1} (Palmer 1991: Fig. 7). Similar autogenic water flowing through calcareous soils with 1 % P_{CO2} continuously maintained in open conditions could saturate at 212 mg L^{-1} before entering the lime-stone. The P_{CO2} of cave air does not normally fall below the level of the surface atmospheric, presently 0.04 %. Water under such conditions saturates at 12 or 68 mg L^{-1} in closed or open conditions, respectively. Assuming degassing occurs under open conditions, drips may thus become aggress-ive, with no deposition, or deposit a maximum of 144 mg of speleothem from each litre of water. Water flowing from a passage via fissures in its floor that drips into a lower passage may experience "prior calcite precipitation" (Fairchild and Baker, 2012, p. 26). It will then become aggressive or deposit speleothem again, depending on the relative P_{CO2} of the cave air in the two passages.

It seems conceivable that dripwaters could achieve chemical breakthrough and then enlarge bedding planes and joints along their flow path, to create explorable passages and shafts. However, the presence of large and old speleothems in many caves suggests that dripwaters enter the limestone nearly saturated and/or flow in long tiny fissures, remaining near saturation for >> 100,000 years. In the competition between the slow enlargement of the dripwater flow path and the lower P_{CO2} level of cave air, degassing should help retain the chemical regime before the drip exit in a pre-breakthrough condition and prolong deposition.

The geometry of dripwater flow paths is never known, and has rarely, if ever, been modelled. Cave air P_{CO2} can vary from dangerous levels of ~5 %, when degassing and deposition are unlikely, to atmospheric levels at cave entrances, where speleothems are commonly located. Nevertheless, dripwaters from cave roofs that follow a vertical path down short joints from a bare limestone surface are more likely to be aggressive and less likely to deposit speleothem, in contrast to those that flow from calcareous soils along longer flow paths with small hydraulic gradients.

Under intermediate conditions, dripwater might become aggressive during floods that raise hydraulic gradients, thereby causing dissolution of speleothem.

During winter, interesting and complex competitions arise among the effects of lower temperature and its consequential reduction of biological activity and therefore of P_{CO2} in dripwaters. Reduced temperature increases the amount of calcite that can be held in solution, thereby increasing penetration lengths and significantly reducing breakthrough times. (However, dissolution rates are significantly reduced after breakthrough). Reduced P_{CO2} levels reduce the calcite saturation level, thereby reducing penetration lengths and increasing breakthrough times (post-breakthrough dissolution rates are also somewhat reduced for applicable ranges of P_{CO2}). Because the temperature change is likely to be damped when the dripwater reaches open cave passage, the change in P_{CO2} is likely to have the major influence. Thus, assuming the dripwater flow always operates with high-order kinetics, i.e. it remains pre-breakthrough, its solute load is reduced and therefore winter precipitation of speleothem should be reduced, at the same flow rate. However, the P_{CO2} of winter cave air may also reduce, increasing precipitation.

13. Speleogenesis below reservoirs and lakes

If the entry to the karst is itself under a head of water, this head needs to be added to the head within the karst to give the applicable hydraulic gradient. Such increased HGs can cause rapid breakthrough by enlargement of karst fractures beneath a reservoir, as studied by Dreybrodt (1996). Thus, a reservoir dam can be bypassed by an underlying conduit, causing significant leakage of the reservoir. Close to the wall of the dam, the HG can exceed unity. For example, from Figure 1, if the leakage is 900 m away and down the valley from a fracture system that leads 100 m below the base of a dam that holds back water 100 m deep, L = 1,000 m and HG = 200/1,000 = 0.2, giving a breakthrough aperture of 0.4 cm. For a 10 m-long sub-horizontal fracture directly beneath the same dam, HG = 10, giving a required aperture of 0.025 cm, so that immediate tectonic inception is likely here. Similar conditions can arise during the deglaciation of continental ice sheets in mountainous areas, if the fractures become submerged by an ice-dammed lake (Faulkner 2005). In this case, the flow path is from the lake and via the fractures back into the lake and then into englacial conduits within the continuing ice sheet, or directly from the fractures into Nye channels at the base of a warm-based ice sheet. Despite the water being at 0 °C, with a P_{CO2} then of only 0.02 %, such situations can also cause tectonic inception and fairly rapid first-order dissolution (Faulkner 2006b).

14. Rejuvenation in alpine situations

Glacial valleys in mountainous areas, including those at high latitudes, were significantly rejuvenated following large-scale erosion during each Pleistocene glaciation. At least the upper and outer parts of palaeocaves may be removed during glacial maxima (Faulkner 2007b). During each ensuing interglacial, sinks may be captured farther upstream and resurgences find lower outlets. Clearly, these effects may make significant changes to hydraulic gradients and hydraulic ratios, depending on the local topography. They provide opportunities for new fractures at lower levels to carry some of the drainage. These may in turn eventually achieve breakthrough and then grow large enough to be explored by diving.

15. Conclusions

The onset of turbulence in a uniform conduit is controlled by two main variables: the aperture (i.e. fissure width or tube radius) and the hydraulic gradient, whereas the onset of first-order kinetics after breakthrough is also controlled by the length of the conduit. Mathematically, hydraulic gradient and length are usefully combined into a single variable, the hydraulic ratio. The two onsets only coincide at the same aperture for planar fissures of length 290 m and for cylindrical tubes of length 452 m, the actual aperture depending on the hydraulic gradient. Thus, breakthrough may occur before or after flow becomes turbulent, depending on conduit length. The time to reach it also depends on three main variables: initial aperture, hydraulic gradient, and conduit length. For many karst aquifers, breakthrough occurs at an aperture of about 1cm for 10 m-long conduits at a hydraulic gradient of 10^{-4} and for longer and steeper conduits up to 1,000 m long at 10^{-2}. However, there are many different karstic situations governed by the same laws. In practice, the breakthrough aperture may vary from the sub-millimetre to several metres and hydraulic ratios can be considered over 17 orders of magnitude.

Acknowledgements

The author is grateful to Art Palmer and Philippe Audra for their suggestions to clarify several points.

References

Bögli A, 1964. Mischungskorrosion – ein Beiträg zur Verkarstungsproblem. Erdkunde, 18, 83–92.

[English translation by Elder E, 1985. Mixture Corrosion – a contribution to the karstification problem. National Speleological Society, Cave Geology, 1 (10), 393–406].

Dreybrodt W, 1990. The role of dissolution kinetics in the development of karst aquifers in limestone: a model simulation of karst evolution. Journal of Geology, 98 (5), 639–655.

Dreybrodt W, 1996. Principles of early development of karst conduits under natural and man-made conditions revealed by mathematical analysis of numerical models. Water Resources Research, 32 (9), 2923–2935.

Dreybrodt W, Gabrovsek F, Romanov D, 2005. Processes of speleogenesis: a modeling approach. Zalozba, ZRC. Postojna – Ljubljana. 376.

Fairchild, IJ, Baker, A, 2012. Speleothem Science. Wiley-Blackwell, 432.

Faulkner TL, 2005. Cave inception and development in Caledonide metacarbonate rocks. PhD Thesis. University of Huddersfield.

Faulkner T, 2006a. Limestone dissolution in phreatic conditions at maximum rates and in pure, cold, water. Cave and Karst Science, 33 (1), 11–20.

Faulkner T, 2006b. Tectonic inception in Caledonide marbles. Acta Carsologica, 35 (1), 7–21.

Faulkner T, 2007a. Book review: Hypogene Speleogenesis: Hydrogeological and morphogenetic perspective by Dr. AB Klimchouk, National Cave and Karst Research Institute Special Paper No. 1, 2007, 106. Cave and Karst Science, 33 (3), 138–141.

Faulkner T, 2007b. The top-down, middle-outwards model of cave development in Caledonide marbles. Cave and Karst Science, 34 (1), 3–16.

Faulkner T, 2009. Limestone erosion rates and rainfall. Cave and Karst Science, 36 (3), 94–95.

Ford DC, Williams P, 2007. Karst hydrogeology and geomorphology, 562. John Wiley and Sons.

Gunn J, Gagen P, 1987. Limestone quarrying and sinkhole development in the English Peak District. in Beck and Wilson (Eds.) Karst hydrogeology, Rotterdam: Balkema, 121–125.

Kaufmann G, Braun J, 1999. Karst aquifer evolution in fractured rocks. Water Resources Research, 35 (11), 3223–3238.

Klimchouk A, 2007. *Hypogene Speleogenesis: Hydrogeological and Morphogenetic Perspective*. National Cave and Karst Research Institute Special Paper No. 1, 106.

Lowe DJ, Gunn J, 1997. Carbonate Speleogenesis: An Inception Horizon Hypothesis. Acta Carsologica, 26/2, 38, 457–488.

Palmer AN, 1981. Hydrochemical factors in the origin of limestone caves. Proceedings of the eighth International Speleological Congress, 120–122.

Palmer AN, 1991. Origin and Morphology of limestone caves. Geological Society of America Bulletin, 103, 1–21, 157–175.

Palmer A, 2007. Cave Geology. Cave Books. Dayton, Ohio. 454.

Romanov D, Gabrovsek F, Dreybrodt W, 2003. The impact of hydrochemical boundary conditions on the evolution of limestone karst aquifers. Journal of Hydrology 276, 240–53.

Weyl PK, 1958. The solution kinetics of calcite. Journal of Geology, 66, 163–176.

White WB, 1977. Role of solution kinetics in the development of karst aquifers. in Tolsen and Doyle (Eds.) International association of Hydrogeologists, Memoirs, 12, 503–517. White WB, 1988. Geomorphology and hydrology of karst terrains. Oxford University Press.